

Real-world vehicle emission factors in Chinese metropolis city—Beijing

WANG Qi-dong¹, HE Ke-bin¹, HUO Hong¹, James Lents²

(1. Department of Environmental Science and Engineering, Tsinghua University, Beijing 100084, China. E-mail: wqdong@pm25.org; 2. CE-CERT, University of California at Riverside, CA 92507, USA)

Abstract: The dynamometer tests with different driving cycles and the real-world tests are presented. Results indicated the pollutants emission factors and fuel consumption factor with ECE15 + EUDC driving cycle usually take the lowest value and with real world driving cycle occur the highest value, and different driving cycles will lead to significantly different vehicle emission factors with the same vehicle. Relative to the ECE15 + EUDC driving cycle, the increasing rate of pollutant emission factors of CO, NO_x and HC are -0.42—2.99, -0.32—0.81 and -0.11—11 with FTP75 testing, 0.11—1.29, -0.77—0.64 and 0.47—10.50 with Beijing 1997 testing and 0.25—1.83, 0.09—0.75 and -0.58—1.50 with real world testing. Compared to the carburetor vehicles, the retrofit and MPI + TWC vehicles' pollution emission factors decrease with different degree. The retrofit vehicle (Santana) will reduce 4.44%—58.44% CO, -4.95%—36.79% NO_x, -32.32%—33.89% HC, and -9.39%—14.29% fuel consumption, and especially that the MPI + TWC vehicle will decrease CO by 82.48%—91.76%, NO_x by 44.87%—92.79%, HC by 90.00%—93.89% and fuel consumption by 5.44%—10.55%. Vehicles can cause pollution at a very high rate when operated in high power modes; however, they may not often operate in these high power modes. In analyzing vehicle emissions, it describes the fraction of time that vehicles operate in various power modes. In Beijing, vehicles spend 90% of their operation in low power modes or decelerating.

Keywords: real-world testing; vehicle emission factors; driving cycle; power modes

Introduction

In recent years, as many measures have been adopted to reduce coal-burning pollution problems in Beijing. This includes converting many high polluting factories to natural gas reducing concentrations of sulfur dioxide (SO₂) and total suspended particulates (TSP) in the air of urban and suburban Beijing. With reduced stationary source emissions, motor vehicles are becoming the major source of CO, HC and NO_x air pollutant emissions. During the 1990s, the average annual vehicle growth rate in Beijing was as high as 17.4% (Fu, 2001). In 1995, the vehicle number in Beijing was 0.905 million, in 1997, 1.04 million, in 2004 the number reached 2.10 million. From 1949 to 1997, the number of vehicles grew from 2300 to 1.04 million; it took 48 years to reach 1st million vehicles in Beijing. But from 1997 to 2003, it only required 6 years to reach the 2nd million. With the improving economy in Beijing even higher vehicle growth rates are anticipated during the early part of the 21st century. Fig.1 shows the growth in the vehicle population in Beijing from 1990 to 2003.

As a result of the rapid growth in the vehicle population, absolute emissions, the vehicular emission contribution rate to air pollution showed a significant increase (Table 1) resulting in increased ambient concentrations of carbon monoxide (CO) and nitrogen oxides (NO_x).

Table 1 shows that the increasing contribution of vehicular emissions will result in a high contribution of vehicle emissions to ambient concentrations (Wang, 2002). Compared to 1995, the proportion of vehicle pollution significantly increased in 1998.

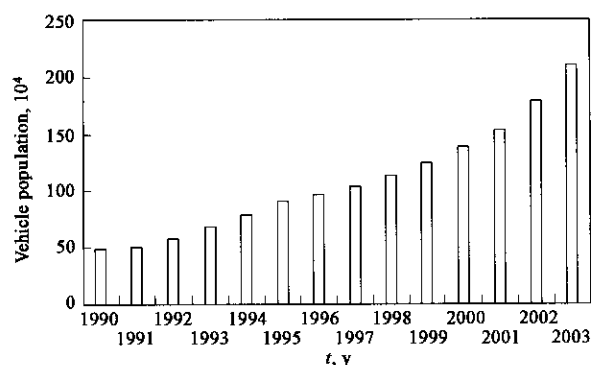


Fig.1 Growth in the vehicle population in Beijing

Table 1 Vehicular emissions and their contribution rate in Beijing

Vehicular emission sources	1995		1998	
	Emission contribution rate, %	Concentration contribution rate, %	Emission contribution rate, %	Concentration contribution rate, %
CO	76.8	76.0	82.7	84.1
NO _x	40.2	68.0	42.9	72.8

As the vehicle population in Beijing is expected to continue to increase at a high rate, there is an urgent need to know that the real-world emission factors and the emission relationships among the different driving cycles, such as European driving cycles: ECE15 + EUDC, American driving cycle: FTP75, Beijing driving cycle: Beijing-1997 and real-world vehicle emission.

1 Vehicle testing

1.1 Test equipment

The real-world vehicle testing equipment used in this

study consists of three parts: OTC microgas analyser, datron GPS instrumentation(Fig.2). system(DFL, MicroStar sensor and software package) and

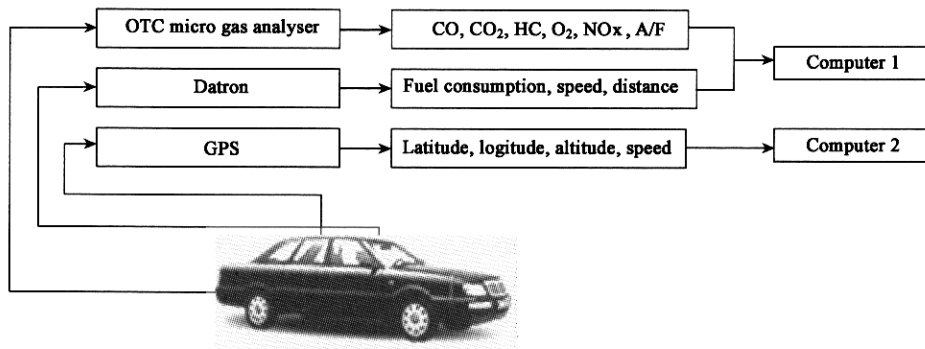


Fig.2 Real-world testing equipment

The OTC microgas is the most compact and accurate 5-gas(HC, CO, CO₂, O₂ and NO_x) analyzer and has BAR 97/ASM approved accuracy. The gas analyzer will test all five-emission gases, plus simultaneously display the air to fuel ratio(A/F).

The DFL flow meter is a compact, easy-to-install unit for measuring fuel consumption. The MicroStar Sensor provides accurate, reliable non-contact speed and distance measurement using technology based on the Doppler principle. For data acquisition of DFL and MicroStar Sensor, the DATRON software package is developed for mobile vehicle testing. After the installation and setup, the Datron

system can display: second by second fuel consumption(L/h) and accumulated fuel consumption (L), second by second speed(km/h), accumulated distance(m).

The GPS instrumentation and a laptop can receive 4—8 satellites in Beijing and can record the vehicle speed on a second by second basis while also providing the position of the vehicle (latitude, longitude and altitude).

1.2 On-road vehicle testing

Eight passenger vehicles were selected for testing. These vehicles included a range of odometer readings, engine size, engine technologies, and control equipment. Specific data on the tested vehicles are shown in Table 2.

Table 2 The brief situation of tested vehicles in Beijing

Testing date	Source fleet	Engine and displacement	Odometer, km	Tech type	GVW	Weather		
						T, °C	Humidity, %	Atm, kPa
3 - 31 - 2003	Beijing	SANTANA GL, 1.8 L(m2)	80100	MPI + TWC	1130	17	53.1	101
4 - 1 - 2003						17.8	59	101.02
4 - 7 - 2003						15.7	44.5	101.14
4 - 8 - 2003	Beijing	Jetta Ci, 1.6 L(m1)	48600	MPI + TWC	1130	19	73	100.75
4 - 14 - 2003						19	32	101.6
4 - 15 - 2003						16.5	39	100.18
6 - 3 - 2003						20	28	99.6
6 - 4 - 2003	Beijing	Jinbei, 2.2 L(m1)	14800	MPI + TWC	1810	17	43	99.8
6 - 5 - 2003						26	48	100.4
6 - 16 - 2003						25.1	48	100.2
6 - 17 - 2003	Beijing	SANTANA, 1.8 L(c2)	98500	Carburetor	1130	31	50	100
6 - 17 - 2003						22	84	100.5
6 - 17 - 2003						26.7		100.1
6 - 20 - 2003						27	43	100.1
7 - 4 - 2003	Beijing	SANTANA, 1.8 L(cr2)	94000	Carburetor retrofit	1130	28.1	44	99.9
7 - 5 - 2003						28	50	99.5
9 - 18 - 2003						34	44	99.5
7 - 5 - 2003	Beijing	Alto, city baby, 0.9 L(m1)	79500	MPI + TWC	680	33	46	99.4
9 - 18 - 2003						31	40	99.3
9 - 18 - 2003	Beijing	Fukang, 1.36 L(m3)	207000	MPI + TWC	1020	34.5	20	99.9
10 - 26 - 2003						25.1	82	101.1
10 - 26 - 2003	Beijing	Jeep, 3.0 L(m1)	50600	MPI + TWC	1930	23.7	79	101.1
10 - 26 - 2003						16.8	36	100.4

Note: m = MPI + TWC; c = carburetor; cr = carburetor retrofit; 1 = odometer less than 80000 km; 2 = 80000 km < odometer < 120000 km; 3 = more than 120000 km

1.3 Test route

The testing route was selected to cover typical roadways

in Beijing (Fig. 3), such as freeways: E-F; arterial roadways: 2nd (H-I), 3rd (D-E) and 4th (F-G) ring

roads, Pingan Avenue (K-L), Zhongguancun Street (A-B); residential roadways: B-C, C-D, G-H, J-K. The whole

testing route is 29.66 km long and covers 4 of 7 urban districts in Beijing.

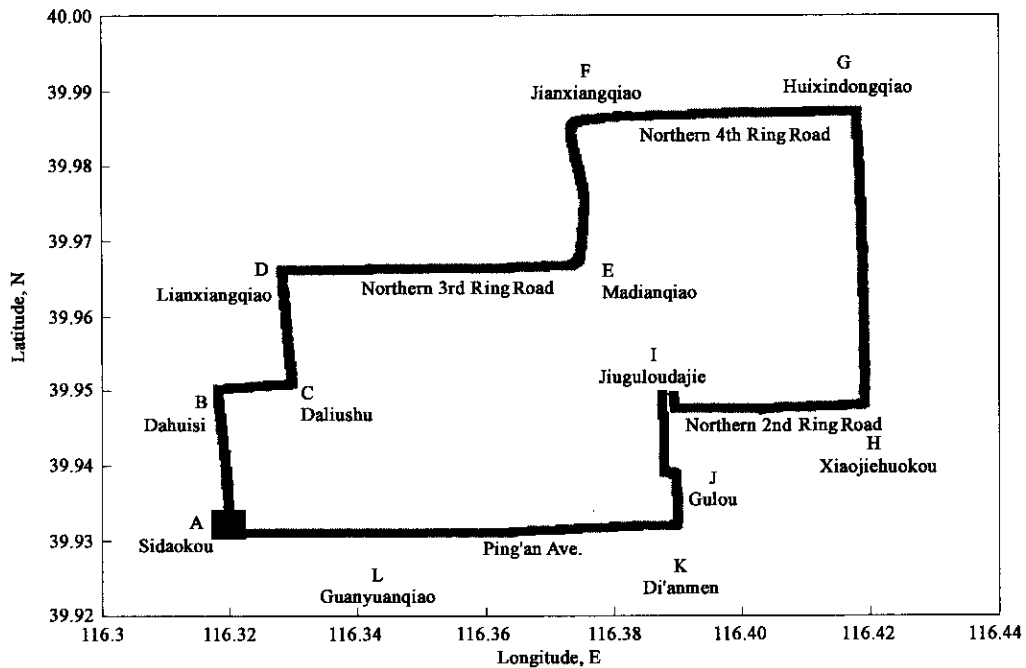


Fig.3 Beijing vehicle testing route

1.4 Data collection

A local professional driver drove the test vehicles, so this can reduce the effect of different driver behaviors. The driver was asked to drive the fixed route that can reflect the whole driving pattern of urban driving in Beijing. The driver drove in the morning, from 7:30 to 9:00 am, 5:00 to 6:30 pm, the rush hour period, and the non-rush hour period, from 11:30 am to 1:00 pm. Following the on-road testing, vehicles were tested on the dynamometer with different driving cycles which include European driving cycle: ECE15 + EUDC, American driving cycle: FTP75 and local Beijing driving cycle: Beijing 1997. Average emission factors with the different driving cycles and for the different vehicles were collected.

2 Methodologies

The data provided by the GPS instrumentation and the Datron system were stored in text files, but the data provided by OTC Microgas Analyser were transferred into excel files after returning from each trip. Several filtering steps were necessary to remove extraneous data, including removing duplicate records and very short files. Then, considering the time lag, we combined GPS second by second data (speed, latitude, longitude and altitude), Datron system second by second data (fuel consumption, accumulated fuel consumption, speed, accumulated distances) and OTC Microgas Analyser data of instantaneous concentrations (HC, CO, CO₂, O₂ and NO_x) to do data processing.

The instantaneous emission rates of HC, CO, CO₂, O₂ and NO_x of the gasoline vehicles (g/s) were calculated by

standard methods described in the SAE Handbook (SAE, 1996). Conversion to mass emission rates—conversion to mass terms should be wet species concentration data, but care must be taken that all data are reported on the same basis. Since engine emissions are discharged to the atmosphere in the wet state, it would seem reasonable to report emissions concentrations on a wet basis. For this reason, the conversion equations and a method for converting dry concentration data into wet terms are given in Appendix 1. The equations for instantaneous mass emission rate (g/s) are shown in the appendix.

Average vehicular emissions and fuel consumption (Tong, 2000) were used to describe emissions and fuel consumption over a trip and were expressed in distance-based unit: g/km and l/100 km. Average emissions, fuel consumption factors were calculated by Equations (1) and Equation (2).

$$\text{Average emission factor (g/km)} = \frac{3600 \times \sum e(\text{g/s})}{\sum v(\text{km/h})}, \quad (1)$$

$$\text{Average fuel consumption factor (l/100 km)} = \frac{100 \times \sum f(\text{L/h})}{\sum v(\text{km/h})}, \quad (2)$$

where e is the second by second emission rates of the subject gas pollutant, f is the second by second fuel consumption rate, and v is the second by second vehicle speed.

Besides global analysis to vehicle emissions, we expect that velocity, acceleration, power requirements, road grade will be considered in the modal analysis. Therefore, the vehicle specific power and engine stress were estimated for

each type of driving. The methodology selected by EPA for the MOVES framework after review of several proposed methods was vehicle specific power (VSP) binning in which emissions are modeled using modal bins and engine stress which is related to vehicle power load requirements and engine RPM (Jose, 1999).

VSP (kW/ton) can be calculated for each second of data using Equation (3):

$$\text{VSP} = v[1.1a + 9.81(a \tan(\sin(\text{grade}))) + 0.132] + 0.000302v^3, \quad (3)$$

where $\text{grade} = (h_{t=0} - h_{t=-1})/v_{(t=-1 \text{ to } 0)}$, v = velocity (m/s), a = acceleration (m/s^2), h = altitude (m).

Engine stress is related to vehicle power load requirements over the past 20 seconds of operation and engine RPM (Equation (4)).

$$\text{Engine stress (unitless)} = \text{RPM index} + (0.08 \text{ ton/kW}) \times \text{preaverage power}, \quad (4)$$

where $\text{preaverage power} = \text{average}(\text{VSP}_{t=-5s \text{ to } -25s})$ (kW/ton); $\text{RPM index} = \text{velocity}_{t=0}/\text{speeddivider}$ (unitless);

minimum RPM index = 0.9.

A total of 60 bins for the VSP/stress categories were used in the analysis (Boundaries assumed in VSP/engine stress binning are shown in appendix). Engine stress is an emissions estimation component developed at the University of California at Riverside to account for emissions that occur at similar power requirements under different engine operating conditions.

3 Results and discussion

3.1 Global analysis results

After on-road testing and laboratory testing on the dynamometer, the average vehicular emission factors and fuel consumption factors were calculated.

3.1.1 The comparison between the same vehicle, different driving cycles

Table 3 shows that the average emission factors and fuel consumption factors compared with the same vehicles, but different driving cycles.

The European driving cycle ECE15 + EUDC is as the

Table 3 Average emission factors and fuel consumption factors comparison with the same vehicles but different driving cycles

Vehicles	Pollutants emission factors and fuel consumption factors	Driving cycles			
		ECE15 + EUDC	FTP75	Beijing 1997	Real world
Alto(m1)*	CO, g/km	1.59	6.34	3.64	3.33
	NOx, g/km	0.80	0.85	1.31	1.24
	HC, g/km	0.16	0.38	0.43	0.40
	Gasoline consumption factors, l/100 km	5.48	8.37	6.64	6.38
Fukang(m3)(taxi)	CO, g/km	4.63	5.87	8.11	10.67
	NOx, g/km	1.00	1.31	0.56	1.09
	HC, g/km	0.59	0.53	1.19	0.25
	Gasoline consumption factors, l/100 km	6.82	8.81	7.76	9.08
Jetta(m1)	CO, g/km	0.68	1.94	1.34	1.57
	NOx, g/km	0.31	0.21	0.07	0.37
	HC, g/km	0.02	0.24	0.23	0.04
	Gasoline consumption factors, l/100 km	8.4	10.21	9.6	9.72
Jeep(m1)	CO, g/km	0.72	0.87	0.81	2.04
	NOx, g/km	1.33	2.41	0.88	2.33
	HC, g/km	0.41	0.62	1.12	0.25
	Gasoline consumption factors, l/100 km	12.73	17.87	14.72	16.98
Petrol van(m1)	CO, g/km	2.84	1.64	3.15	3.54
	NOx, g/km	0.07	0.06	0.05	0.09
	HC, g/km	0.19	0.17	0.28	0.22
	Gasoline consumption factors, l/100 km	11.89	14.14	11.39	12.66

Note: * m1—expressing that the test vehicles' technology types belong to multi-point injection, and odometer less than 80000 km; 3 = more than 120000 km

standard driving cycle in China, so we regard vehicles at ECE15 + EUDC driving cycle as the base emission factor and base fuel consumption factor, the ratios of emission factors and fuel consumption of other driving cycles are shown in Table 4. Table 4 shows that the pollutants emission factors and fuel consumption factor with ECE15 + EUDC driving cycle usually take the lowest value and with real world driving cycle occur the highest value.

3.1.2 Comparison between the same brand vehicles, different engine technology types

Table 5 shows that the comparison of average emission factors and fuel consumption factor among the same brand vehicles (different vehicles) but different in engine technology types.

3.1.3 Discussion

Through comparing, we can find that the vehicle emission factors are quite different with the same vehicle at different driving cycles and the same driving cycle with different vehicles. Relative to the ECE15 + EUDC driving cycle, the increasing rate of pollutant emission factors of CO,

Table 4 The increasing rates of emission factors and fuel consumption factor of the various driving cycles compared to the ECE15 + EUDC driving cycles

Vehicles	Pollutants and fuel consumption factors	ECE15 + EUDC- based, g/km	Increasing rate relative to ECE15 + EUDC		
			FTP75	Beijing 1997	Real world
Alto(m1) *	CO	1.59	2.99	1.29	1.09
	NOx	0.80	0.06	0.64	0.55
	HC	0.16	1.38	1.69	1.50
	Gasoline consumption	5.48	0.53	0.21	0.16
Fukang(m3)(taxi)	CO	4.63	0.27	0.75	1.30
	NOx	1.00	0.31	-0.44	0.09
	HC	0.59	-0.10	1.02	-0.58
	Gasoline consumption	6.82	0.29	0.14	0.33
Jetta(m1)	CO	0.68	1.85	0.97	1.31
	NOx	0.31	-0.32	-0.77	0.19
	HC	0.02	11.00	10.50	1.00
	Gasoline consumption	8.40	0.22	0.14	0.16
Jeep(m1)	CO	0.72	0.21	0.13	1.83
	NOx	1.33	0.81	-0.34	0.75
	HC	0.41	0.51	1.73	-0.39
	Gasoline consumption	12.73	0.40	0.16	0.33
Petrol van(m1)	CO	2.84	-0.42	0.11	0.25
	NOx	0.07	-0.14	-0.29	0.29
	HC	0.19	-0.11	0.47	0.16
	Gasoline consumption	11.89	0.19	-0.04	0.06

Table 5 The same brand vehicles' (Santana) emission factors with different engine tech types

Pollutants emission factors and fuel consumption factors	Driving cycles	Vehicles			Based on Santana (c2), the decreasing rate, %	
		Santana (c2)	Santana(cr2)	Santana(m2)	Santana(cr2)	Santana(m2)
CO, g/km	ECE15 + EUDC	25.40	16.19	3.68	-36.26	-85.51
	FTP75	29.49	26.85	4.94	-8.95	-83.25
	Beijing 1997	40.54	16.85	3.34	-58.44	-91.76
	Real world	41.62	39.77	7.29	-4.44	-82.48
NOx, g/km	ECE15 + EUDC	2.22	2.33	0.16	4.95	-92.79
	FTP75	1.56	1.50	0.86	-3.85	-44.87
	Beijing 1997	0.62	0.65	0.25	4.84	-59.68
	Real world	1.06	0.67	0.58	-36.79	-45.28
HC, g/km	ECE15 + EUDC	1.80	1.19	0.11	-33.89	-93.89
	FTP75	1.98	2.62	0.14	32.32	-92.93
	Beijing 1997	2.28	2.10	0.20	-7.89	-91.23
	Real world	0.80	0.92	0.08	15.00	-90.00
Gasoline consumption factors, l/100 km	ECE15 + EUDC	8.46	8.21	7.81	-2.96	-7.68
	FTP75	10.14	10.54	9.14	3.94	-9.86
	Beijing 1997	9.38	8.04	8.39	-14.29	-10.55
	Real world	9.37	10.25	8.86	9.39	-5.44

NOx and HC are -0.42—2.99, -0.32—0.81 and -0.11—11 with FTP75 testing, 0.11—1.29, -0.77—0.64 and 0.47—10.50 with Beijing 1997 testing and 0.25—1.83, 0.09—0.75 and -0.58—1.50 with real world testing. Moreover, the increasing rate of fuel consumption factor is 0.19—0.53 at FTP75, -0.04—0.21 at Beijing 1997 and 0.25—12.66 at real world testing. A key reason for the difference is that driving cycle is an important factor impacting vehicle emissions, such as the amount of idle, acceleration, deceleration and cruising speed, and so on (Table 6). The second reason is that the ECE15 + EUDC driving cycle is regarded as the standard driving cycle.

Therefore, the manufacturers will adjust the vehicle engines to fit well for the standard driving cycle for new produced vehicles type approval test and conformity inspection, so the vehicles emission factors with ECE15 + EUDC driving cycle is the lowest. The third reason is that the Beijing 1997 driving cycle was developed in 1997 and is not representative of the driving in Beijing today because of the much larger number of vehicles in operation on Beijing roads. Although the emission resulting from the Beijing driving cycle is the closest of the driving cycles studied on the present on-road emissions measured in this study.

Table 6 Modes analysis of different driving cycles

Driving cycle	Simulated distance, km	Average speed, km/h	Maximum speed, km/h	Idle, %	Acceleration, %	Deceleration, %	Cruise, %
ECE15 + EUDC	11.007	33.2	120	25.15	26.58	18.09	29.37
FTP75	17.86	31.5	91.2	19.02	35.57	29.52	15.89
Beijing 1997	5.697	19.2	65.1	19.44	31.31	36.36	12.90
Beijing 2003	6.382	20.39	91.1	21.47	33.27	34.16	11.09
Real world	401.652	20.5	73.2	21.11	33.42	33.37	12.10

Table 5 shows that the retrofit vehicle (Santana) will reduce 4.44%—58.44% CO, - 4.95%—36.79% NO_x, - 32.32%—33.89% HC and - 9.39%—14.29% fuel consumption, and especially that the MPI + TWC vehicle will decrease CO by 82.48%—91.76%, NO_x by 44.87%—92.79%, HC by 90.00%—93.89% and fuel consumption by 5.44%—10.55%. These on-road testing results proved that it is essential to retrofit carburetor vehicles and it is ideal way to improve engine technology types for pollutants' reduction.

As noted earlier, the vehicle emission factors are quite different with different driving cycles and different vehicle technology. We need to update the Beijing vehicle emission factors when we want to calculate or predict total vehicle emission amounts in the city. Otherwise, the results will be inaccurate.

3.2 Modal analysis results

VSP has been used as a power surrogate in several previous efforts, and current research projects at the College of Engineering Center for Emissions Reduction and Technology (CE-CERT) at the University of California at Riverside have found that vehicle power-based emissions estimates perform quite well. An additional factor called engine stress is used to supplement VSP to improve emission estimates. Lower engine stress refers to conditions in which vehicle operation has encountered low speed and accelerations over the last 20 s of operation and the engine RPM is relatively low, and high engine stress occurs at high speed and accelerations over the most recent 20 s and engine RPM is high. To account for the impact of VSP and Engine Stress on vehicle emissions a total of 60 bins for the VSP/engine stress categories have been found to be effective to show the vehicle emission characteristics. The data measured in this study were broken into the 60 VSP/Stress bins suggested by the CE-CERT studies. Fig. 4, 5, 6, 7 and 8 show the fraction of driving percentage (abbreviated: FD%) and pollutants (CO, CO₂, NO_x and HC) emission rates as the functions of VSP and engine stress. In general, as congestion increases, the fraction of travel in the lower stress (bin No. 0—19) categories increases. Table 7 illustrates the distribution (percentage) of emission amounts with different engine stresses (low stress: engine stress from - 1.6 to 3.1 (bin No. 0—19); moderate stress: engine stress from 3.1 to 7.8 (bin No. 20—39); high stress: engine stress from 7.8 to 12.6 (bin No. 40—59)).

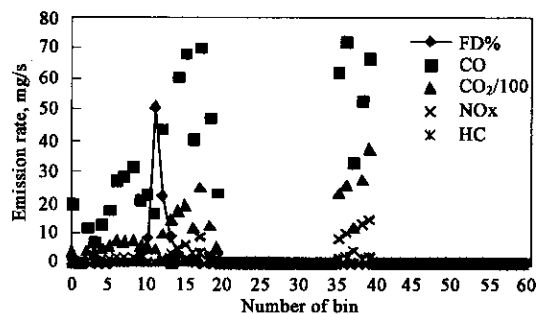


Fig. 4 Alto FD% and pollutants emission rates

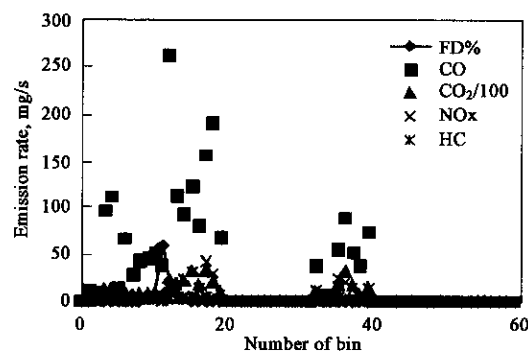


Fig. 5 Fukang FD% and pollutants emission rates

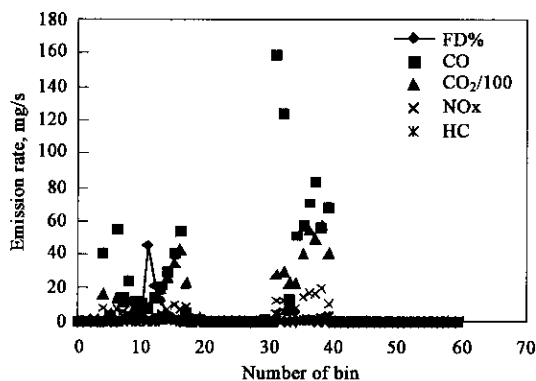


Fig. 6 Jetta FD% and pollutants emission rates

After data analysis and calculation, we can find that the fractions of driving (%) with different vehicles are similar, but the emission rates are quite different. Furthermore, we can find that the biggest fraction of driving appears at bin 11, and emission rates at moderate engine stress sometimes higher than at low engine stress. The bin emission amounts have not only relationship with bin emission rate, but also with the fraction of driving (FD%). Though the biggest fraction of driving locates at bin 11, the biggest emission amounts are

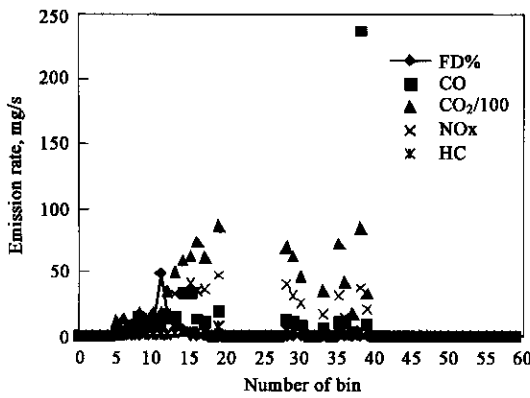


Fig.7 Jeep FD% and pollutants emission rates

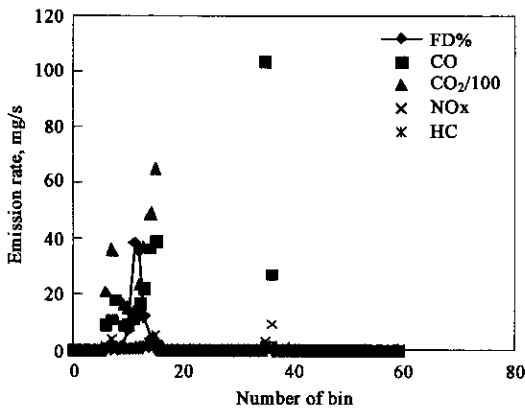


Fig.8 Petrol van FD% and pollutants emission rates

Table 7 The distribution (percentage) of emission amounts with different engine stresses

Vehicles	Pollutants	Emission amounts percentage of engine stress, %		
		Low stress	Moderate stress	High stress
Alto (m1)	CO	99.03	0.97	0.00
	NOx	97.72	2.28	0.00
	HC	99.07	0.93	0.00
Fukang (m3) (taxi)	CO	99.18	0.82	0.00
	NOx	97.68	2.32	0.00
	HC	98.85	1.15	0.00
Jetta(m1)	CO	91.30	8.70	0.00
	NOx	91.66	8.34	0.00
	HC	92.84	7.16	0.00
Jeep(m1)	CO	95.82	4.18	0.00
	NOx	97.86	2.14	0.00
	HC	97.34	2.66	0.00
Petrol van(m1)	CO	98.46	1.54	0.00
	NOx	98.04	1.96	0.00
	HC	99.15	0.85	0.00

not always at bin 11, sometimes at bin 12. In addition, although the moderate stress owns relatively high emission rates, the emission amounts at moderate engine stress only account for around 3%. The reason is that the fraction of driving (FD%) at moderate engine stress only occupies around 1%, but the fraction of driving at low stress in Beijing occupies around 99%. This can be expressed that

vehicle operation has encountered low speed and accelerations over the last 20 s of operation and the engine RPM is relatively low. This means that vehicles driving pattern is not ideal and needs to be improved.

Through vehicles' modal driving analysis, we can build the database of the different vehicles emission rates with different bins in Beijing. Data can also be drawn from the database of modal emission models, such as CMEM (comprehensive modals of emission models), IVE (International vehicle emission) models. It is better to use the appointed city's database for model to calculate the appointed city's emission factors, the results will be more close to the real world emission factors and improve the model's reliability.

4 Conclusions

Different driving cycles will lead to quite different vehicle emission factors with the same vehicle. Relative to the ECE15 + EUDC driving cycle, the increasing rate of pollutant emission factors of CO, NOx and HC are -0.42—2.99, -0.32—0.81 and -0.11—11 with FTP75 testing, 0.11—1.29, -0.77—0.64 and 0.47—10.50 with Beijing 1997 testing and 0.25—1.83, 0.09—0.75 and -0.58—1.50 with real world testing. Moreover, the increasing rate of fuel consumption factor is 0.19—0.53 at FTP75, -0.04—0.21 at Beijing 1997 and 0.25—12.66 at real world testing.

Compared to the carburetor vehicles, the retrofit and MPI + TWC vehicles' pollution emission factors decrease with different degree. The retrofit vehicle (Santana) will reduce 24.44%—58.44% CO, -4.95%—36.79% NOx, -32.32%—33.89% HC and -9.39%—14.29% fuel consumption, and especially that the MPI + TWC vehicle will decrease CO by 82.48%—91.76%, NOx by 44.87%—92.79%, HC by 90.00%—93.89% and fuel consumption by 5.44%—10.55%. These on-road testing results prove that it is essential to retrofit carburetor vehicles and it is ideal way to improve engine technology types for pollutants' reduction.

After modal analysis of vehicles, it is found that the fractions of driving (%) with different vehicles are similar, but the emission rates are quite different. Furthermore, we can find that the biggest fraction of driving appears at bin 11, and emission rates at moderate engine stress sometimes higher than at low engine stress. The bin emission amounts have not only relationship with bin emission rate, but also with the fraction of driving (FD%). Although the biggest fraction of driving locates at bin 11, the biggest emission amounts are not always at bin 11, sometimes at bin 12. In addition, although the moderate stress owns relatively high emission rates, the emission amounts at moderate engine stress only account for around 0.85%—8.70%. The reason is that the fraction of driving (FD%) at moderate engine stress and low stress occupies separately around 1% and 99% in Beijing,

but in California, USA, they will be instead about 20% and 80% (Steven, 2002). This can be expressed that vehicle operation has encountered low speed and accelerations over the last 20 s of operation and the engine RPM is relatively low. This means that vehicles driving pattern is not ideal and need to be improved.

It should be noted in concluding that data from only five vehicles were collected. The data demonstrate the relevance of driving cycle and vehicle technology to vehicle emissions. Further data should be collected on multiple vehicles of each technology to properly establish driving cycle/emission relationships.

Appendix:

I Calculation of mass emissions in g/s (gasoline vehicles)

The mass emission rates of CO, HC and NOx for gasoline vehicles in g/s were calculated by the following equations:

$$\text{CO}(\text{mg/s}) = \text{Fuel}(\text{L/s}) \times p(\text{g/L}) \times (1 + A/F) \times M_{\text{CO}} / M_{\text{EXH}} \times K \times X_{\text{COd}} \times 1000 / (3600 \times 100);$$

$$\text{NOx}(\text{mg/s}) = \text{Fuel}(\text{L/s}) \times p(\text{g/L}) \times (1 + A/F) \times M_{\text{NOx}} / M_{\text{EXH}} \times K \times X_{\text{NOxd}} \times 1000 / (3600 \times 10^6);$$

$$\text{HC}(\text{mg/s}) = \text{Fuel}(\text{L/s}) \times p(\text{g/L}) \times (1 + A/F) \times M_{\text{HC}} / M_{\text{EXH}} \times K \times X_{\text{HCd}} \times 1000 / (3600 \times 10^6);$$

$$M_{\text{EXH}} = \frac{13.88 \times K \times X_{\text{HCd}} \text{Cl}}{10^6} + \frac{28.01 \times K \times X_{\text{COd}}}{10^2} + \frac{44.04 \times K \times X_{\text{CO}_2\text{d}}}{10^2} + \frac{46.01 \times K \times X_{\text{NO}_2\text{d}}}{10^6} + \frac{32.00 \times K \times X_{\text{O}_2\text{d}}}{10^2} + \frac{2.016 \times K \times X_{\text{H}_2\text{d}}}{10^2} + 18.01 \times (1 - K) + \left\{ 28.01 \times \left[100 - \frac{K \times X_{\text{COd}}}{10^4} - K \times X_{\text{COd}} - K \times X_{\text{CO}_2\text{d}} - \frac{K \times X_{\text{NO}_2\text{d}}}{10^4} - K \times X_{\text{O}_2\text{d}} \right] - (K \times X_{\text{H}_2\text{d}}) - 100 \times (1 - k) \right\}.$$

Of all:

$$K = \frac{1}{1 + 0.005 \times (X_{\text{COd}} + X_{\text{CO}_2\text{d}}) \times \gamma - 0.01 \times X_{\text{H}_2\text{d}}},$$

$$X_{\text{H}_2\text{d}} = \frac{0.5 \times \gamma \times X_{\text{COd}} \times (X_{\text{COd}} + X_{\text{CO}_2\text{d}})}{X_{\text{COd}} + 3 \times X_{\text{CO}_2\text{d}}}.$$

Where: p = fuel density, g/L; M_{CO} = molecular weight of CO = 28.01; M_{NOx} = molecular weight of NO₂ (NOx) = 46.01; M_{HC} = molecular weight of HC = 13.88; M_{EXH} = average molecular weight of tail exhaust gas; A/F = air and fuel ratio; K = the correction factor to be used in converting dry measurements to a wet basis; X_{COd} = CO concentration (%) on a dry basis; X_{NOxd} = NOx concentration (ppm) on a

dry basis; X_{HC} = HC concentration (ppm) on a dry basis; $X_{\text{O}_2\text{d}}$ = O₂ concentration (%) on a dry basis; $X_{\text{CO}_2\text{d}}$ = CO₂ concentration (%) on a dry basis; $X_{\text{H}_2\text{d}}$ = residual H₂ concentration (%) on a dry basis; γ = H/C atomic ratio of test fuel.

II Boundaries assumed in VSP/engine stress binning (James Lents, 2002)

A total of 60 bins for the VSP/stress categories are as the follows.

Bin	VSP (kW/ton)		Engine stress	
	Lower	Upper	Lower	Upper
0	-80.0	-44.0	-1.6	3.1
1	-44.0	-39.9	3.1	7.8
2	-39.9	-35.8	7.8	12.6
3	-35.8	-31.7		
4	-31.7	-27.6		
5	-27.6	-23.4		
6	-23.4	-19.3		
7	-19.3	-15.2		
8	-15.2	-11.1		
9	-11.1	-7.0		
10	-7.0	-2.9		
11	-2.9	1.2		
12	1.2	5.3		
13	5.3	9.4		
14	9.4	13.6		
15	13.6	17.7		
16	17.7	21.8		
17	21.8	25.9		
18	25.9	30.0		
19	30.0	1000.0		

Note: The bins from 20 to 39 and 40 to 59 will repeat the bins from 0 to 19

References:

- Fu L X, Hao J M, He D Q *et al.*, 2001. Assessment of vehicular pollution in China[J]. Journal of the Air & Waste Management Association, 51: 658–668.
- Wang Q D, He K B, Li T J *et al.*, 2002. Strategies for controlling pollution from vehicular emissions in Beijing[M]. In: Sustainable urban road transport and the greening of auto industry in China (Zhang X. ed.). Beijing: China Environmental Science Publishing Co.
- SAE, 1996. Test procedure for the measurement of gaseous exhaust emissions from small utility engines[M]. SAE J1088 FEB93, 1996 SAE Handbook, 1: Materials, fuels, emissions and noise. Society of Automotive Engineers.
- Tong H Y, Hung W T, Cheung C S, 2000. On-road motor vehicle emissions and fuel consumption in urban driving conditions[J]. Journal of Air & Waste Management Association, 50: 543–554.
- Jose Luis Jimenez-Palacios, 1999. Understanding and quantifying motor vehicle emissions with vehicle specific power and TILDAS remote sensing[D]. Ph D dissertation. Massachusetts Institute of Technology. 54–61.
- Steven H C, 2002. Real-world vehicle emissions; a summary of the eleventh coordinating research council on-road vehicle emissions workshop [J]. Journal of the Air & Waste Management Association, 52: 220–236.
- James L, 2002. Characterization of driving behavior and emissions from on-road vehicles[R]. In: Reports on the development of the IVE model and data collected in Santiago, Chile and Nairobi, Kenya (Nicole Davis ed.). Riverside: University of California at Riverside.